Active Voltage Control (AVC) For Reducing Three-phase Voltage Fluctuations

Pham Thi Giang[1], Nguyen Hoang Duy[2], and Vo Thanh Ha[3*]

[1] Faculty of Electrical Engineering University of Economics-Technology for Industries Hanoi, Vietnam
[2] Faculty of Electrical and Electrical Engineering, Hanoi University of Science and Technology
[3] Faculty of Electrical and Electrical Engineering, University of Transport and Communications, Hanoi, Vietnam
[*] Corresponding author. E-mail: vothanhha.ktd@utc.edu.vn

Received: July 07, 2022; Accepted: December 12, 2022

The paper presents an active voltage compensator (AVC) to prevent voltage fluctuations on the load in both voltage's rise and fall directions. This AVC is designed based on modeling a three-phase four-branch inverter according to the large-signal average model and the small-signal model—calculation and design of d-q channel controller and 0 channel controller by the frequency-domain method. This AVC significantly reduces production interruptions while protecting equipment life reduction. The theory results are proven through MATLAB/Simulink simulation.

Keywords: UPS; AVC; Sag Fighter; Active filtering

http://dx.doi.org/10.6180/jase.202402_27(2).0008

1. Introduction

During the operation of power plants, short-term voltage fluctuations often appear on the grid [1, 2]. This phenomenon is usually caused by reasons such as switching off the compensating capacitor system on the transmission line [3, 4], and [5], or the operation of nonlinear solid loads (typically electrical smelting systems) [6]. Short-term voltage fluctuations usually include a voltage drop of less than 500ms, after which the voltage will recover, but this recovery will always exceed the rated value,e, and the voltage will fluctuate before stabilizing again [7]. Overcoming these short-term voltage fluctuations often requires synchronous implementation of load management measures and installation on the transmission system of electronic power compensation and filtering devices [8]. Accordingly, the loads that generate many current harmonics will not be eligible to connect to the power grid, and the causes caused by the transmission system itself will be suppressed by electronic compensating and filtering devices. However, at present and shortly, the power grid has not overcome this problem [9]. Currently, there are many technical solutions to prevent short-term voltage fluctuations, such as active filtering, uninterruptible power supply (UPS), voltage drop protection (Sag Fighter), and dynamic voltage compensator (AVC).

According to the document [10], active filtering will filter the current harmonics caused by nonlinear loads. In addition to screening for sinusoidal currents, active filters also can balance phases in case of out-of-phase loads, thus potentially increasing the energy efficiency of the system. It can only filter the harmonics generated by loads of the current system but cannot filter the harmonics caused by other loads outside the grid. Besides, the uninterruptible power supply (UPS) will power the essential loads not directly from the grid but the semiconductor inverter. Therefore, it can be said that the voltage quality entirely depends on the power supply and voltage quality generated by the UPS. The induced voltage of the UPS is isolated from the mains voltage by an intermediate direct current (DC) circuit with a battery array connected to it, so the effects of mains voltage variation are automatically compensated by

this battery system. Therefore, the voltage supplied to the load will altogether avoid the impact of grid voltage variation, even if the mains power is completely lost, the UPS can still maintain the voltage supplied to the load from a few minutes to several hours ten minutes depending on the capacity of the batteries [11, 12], and [13].

Based on [14], due to voltage sags, the UST SagFighter TM guards against expensive production halts and manufacturing mistakes. All continuous manufacturing processes and other power-critical applications are provided with essential protection, which may be tailored to satisfy engineering requirements. SagFighter's operational and thermal management expenses are reduced compared to a similar UPS, thanks to its real efficiency of more than 99%. However, maintaining the UPS is costly. It may have a real operational efficiency of less than 95% at absolute input voltage and current draw.

In addition, the active voltage compensator (AVC) is an improvement of the surge suppressor both in terms of the power circuit and control technique shown in Figure 1. This unit is used with controlled active rectification with converters using IGBT. Energy is transferred in both directions, thus enabling load protection against mains voltage variations in both rising and falling demands. Applying new control techniques also allows the AVCs to perform better than the surge suppressors. In particular, it is permitted to compensate when the grid voltage is below 10% of the rated voltage (keep 60% of the voltage) when the 2-phase voltage drops and to 40% when the voltage drops evenly in all three phases (save 70% voltage). The online operation of the AVC also allows its response to be faster and keeps the voltage across the load virtually unchanged [14, 15], and [16].

Thereby finding that the active filter has the best performance characteristics in the voltage compensation solutions mentioned above, the thesis chooses the answer using the dynamic voltage compensator (AVC) [17]. The AVC will prevent voltage fluctuations on the load in both voltage's rise and fall directions, thus ensuring a significant reduction in production interruptions and protecting equipment from shortening its life. Furthermore, the breakdown statistics and capabilities of the AVC unit show that up to 96% reduction in disruption due to voltage fluctuations can be achieved. The AVC active voltage compensator structure consists of a rectifier, an inverter, and an LCL filter. In which a 3-phase diode bridge rectifier is selected to generate a voltage on the DC bus, an inverter with a three-phase four-branch inverter structure [18, 19], and [20].

This paper will be presented in 5 parts. Section 1 provides a general introduction to the field of research on methods of anti-voltage dynamics. Part 2 will introduce the vector modulation algorithm. Then, part 3 designs a voltage controller in the frequency domain. The following section will give simulation results. Finally, evaluate the results obtained in the concluding paragraph.

2. Modeling a three-phase four-branch inverter

2.1. Big signal averaging model

For the sake of modeling, assume that the semiconductor valves are ideally locked. 1 - on, 0 - off. At this time, there is a switch lock diagram as follows:

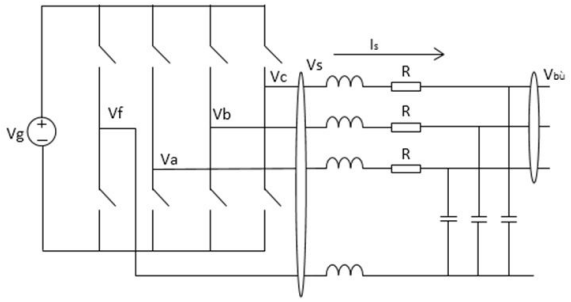

Fig. 1. Location of the KVMRT project

The model in the $dq0$ coordinate system is as follows:

$$\frac{d}{dt}\begin{bmatrix} I_d \\ I_q \\ I_0 \end{bmatrix} = \mathrm{V}_{gG}\begin{bmatrix} d_d \\ d_q \\ d_0 \end{bmatrix} + \mathrm{G}\begin{bmatrix} V_d \\ V_q \\ V_0 \end{bmatrix} + \omega\begin{bmatrix} I_d \\ -I_q \\ 0 \end{bmatrix}$$
$$\mathrm{G} = \begin{bmatrix} \frac{1}{L} & 0 & 0 \\ 0 & \frac{1}{L} & 0 \\ 0 & 0 & \frac{1}{L+3L_n} \end{bmatrix} \tag{1}$$

Where: d_a, d_b, and d_c are the modulation ratio of the valve branches. I_d, I_g, and I_0 are currents in coordinates dq 0 V_d, V_q, and V_0 are voltages in coordinates dq 0 L, Ln is Inductance ; n^{th} inductance G is system matrix

2.2. Small signal pattern

For zero derivative variables $(\dot{X} = 0)$ we find the steady-state values of the signals:

$$\begin{bmatrix} D_d \\ D_q \\ D_0 \end{bmatrix} = \frac{L\omega}{V_g}\begin{bmatrix} -I_{Ld} \\ I_{Lq} \\ 0 \end{bmatrix} + \frac{V_{\mathrm{ln\_}pk}}{V_g}\begin{bmatrix} 1 - LC\omega^2 \\ 0 \\ 0 \end{bmatrix} \tag{2}$$

Where: $V_{\mathrm{ln\_pk}}$: is eactive voltage; C is capacitor; Linearization around the equilibrium working point with small fluctuations: $x = \hat{x} + X$ from which a small signal model AC will be obtained.

3. Designing a voltage controller in the frequency domain

From the AC small-signal model (Figure 3), if the interleaving component is omitted, the AC small-signal model can be considered as three DC - DC buck converters. Therefore, it is possible to apply the controller design for the DC - DC buck converter. The structure of the lead-lag compensator has the following form:

$$G_c(s) = K_c \frac{\left(1+\frac{s}{\omega_z}\right)}{\left(1+\frac{s}{\omega_p}\right)}\left(1+\frac{\omega_L}{s}\right) \quad (3)$$

In there, ω_z and ω_p is determined by the following formula for determining the zero and pole frequencies of the compensator and ω_L will be select by $\frac{f_c}{20}$.

$$\begin{cases} f_z = f_c\sqrt{\frac{1-\sin\theta}{1+\sin\theta}} \\ f_p = f_c\sqrt{\frac{1+\sin\theta}{1-\sin\theta}} \end{cases} \quad (4)$$

3.1. Calculation of channel controller d-q

As stated above, the paper will choose the phase and fL margin of 55° and $\frac{f_c}{20}$, respectively. Based on the calculated parameters, give the bode graph of the transfer function $G_{qd}(s)$ as follows:

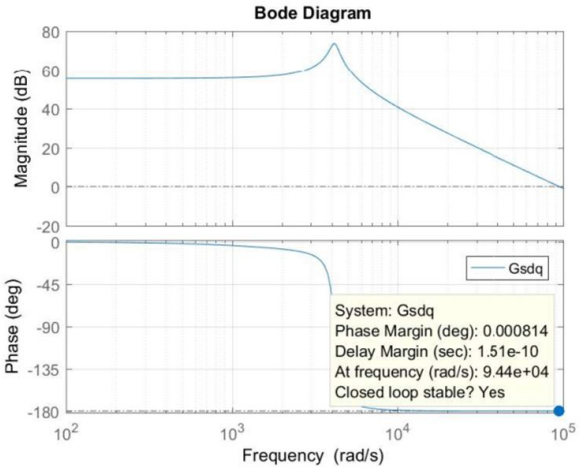

Fig. 2. Bode graph of transfer function $G_{qd}(s)$.

Figure 2 shows that the phase reserve is currently only, and the cutoff frequency is approximately 95kHz. From there, design the controller so that the phase reserve is increased. With $\theta_{PM} = 55°$ and the transfer function phase reserve is $\theta_{DT} = 0.00152°$ so the controller phase will be substituting numbers into Eq. (4) will get the frequency:

$$\begin{cases} f_z = 3.1533\text{kHz} \\ f_p = 31.713\text{kHz} \end{cases}$$

K_c will be calculated according to the following formula: $\frac{1}{m_{ag_1 \cdot mag_2}}$ (Where mag_1 and mag_2 are the phase reserve of the object, the controller and calculated through the MATLAB function will be mentioned in the appendix). According to calculation $K_c = 0.1392$.

Bode graph of the object after having the controller:

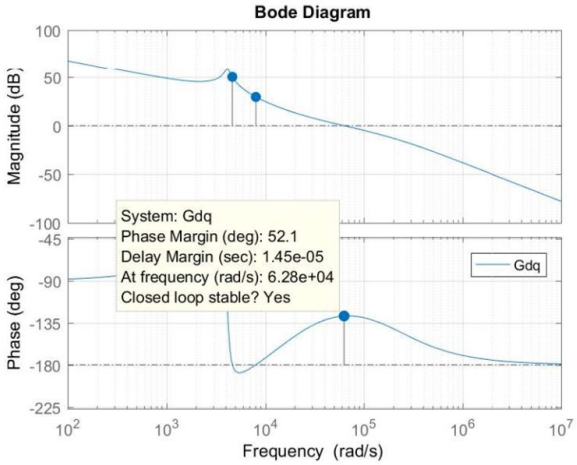

Fig. 3. Bode plot after having the controller of the $d-q$.

We see that the phase reserve achieved is 52.1^0 (meeting design requirements). Therefor, the paper will use the above controller for simulation.

3.2. Channel controller calculation 0

Following is the bode plot of the transfer function $G_0(s)$:

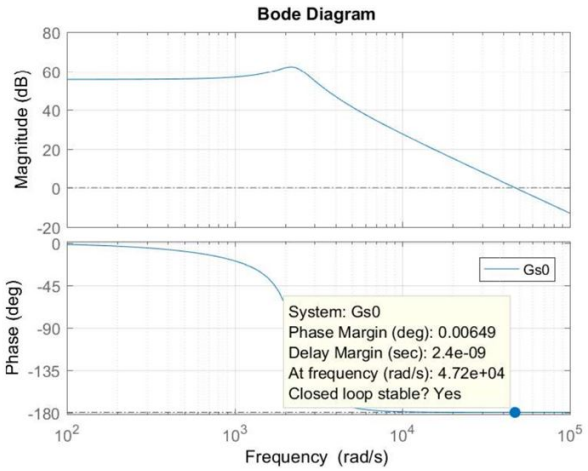

Fig. 4. Bode graph of transfer function $G_o(s)$ without controller.

From the graph, it can be seen that the phase reserve has and the cutoff frequency is 47 kHz. Next will increase

the phase reserve thanks to the controller, obtaining:

$$\begin{cases} f_z = 3.1532\text{kHz} \\ f_z = 31.714\text{kHz} \\ K_c = 0.5584 \end{cases}$$

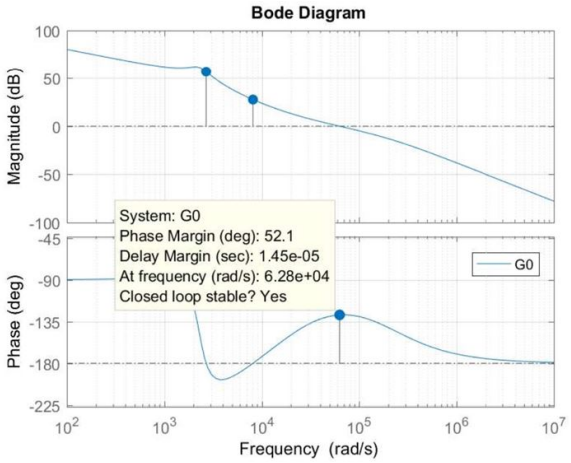

Fig. 5. Channel 0 object transfer function after having controller.

The achieved phase reserve is 52.1° (meeting design requirements). So will use the above controller to simulate.

4. Simulation results

This paper uses MATLAB/Simulink to simulate a 3-phase voltage compensation system using a 3-phase 4-branch inverter structure. Build a voltage compensator simulation model with:

- Rated load capacity 10KVA
- 3-phase voltage source rated voltage 311V, frequency 50Hz
- Load RL, Diode
- THD output voltage < 3% (for balanced loads), < 5% (for nonlinear and unbalanced loads)
- Ability to compensate when 3-phase voltage depression occurs to 70%: >90%
- Ability to compensate when 1-phase voltage depression occurs to 50%: >90%
- Ability to compensate when voltage convex in 1 phase at 115%: 100%

The controller structure is shown in Figure 6:

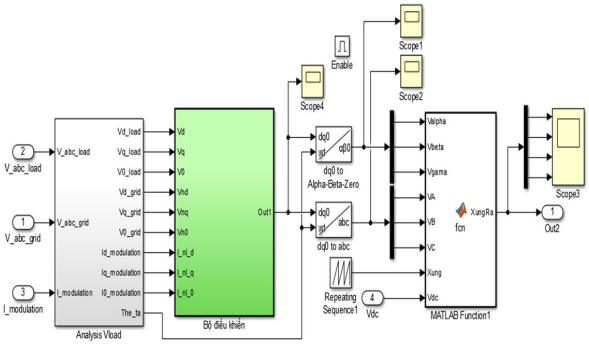

Fig. 6. Controller structure.

4.1. Case of voltage sag

Assume that the voltage across phase A drops by 100V, phase B drops by 100V, and phase C drops by 50V

4.1.1. In case of resistive load R = 100R balanced

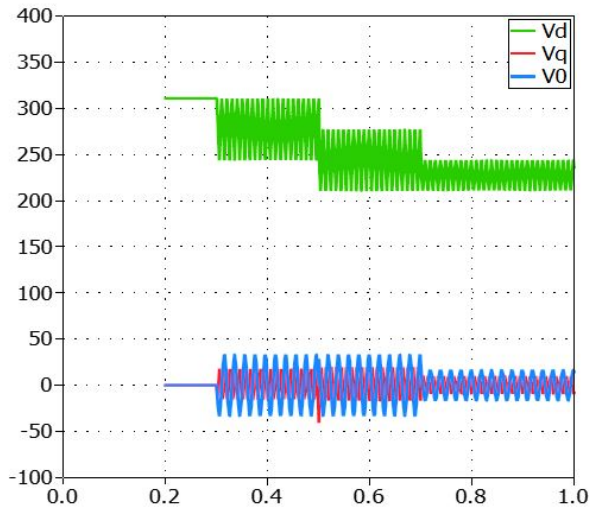

Fig. 7. Grid voltage on the coordinate system dq0.

With resistive load, when voltage variation occurs, $dq0$ components will fluctuate. With impact compensation, components dq0 return to 1-way value with component d equal to the rated voltage value and all components q equal to 0.

Compensator performance is good, with voltage variations in 1-phase to 3-phase drops. The value of the voltage after compensation satisfies the requirements outlined in amplitude and frequency.

4.1.2. In case of nonlinear load (diode bridge)

For nonlinear loads, the ratio of the high-order harmonics is high, so the offset voltage signals on the dq0 coordinate system cannot reach the desired 1-way value. The controller

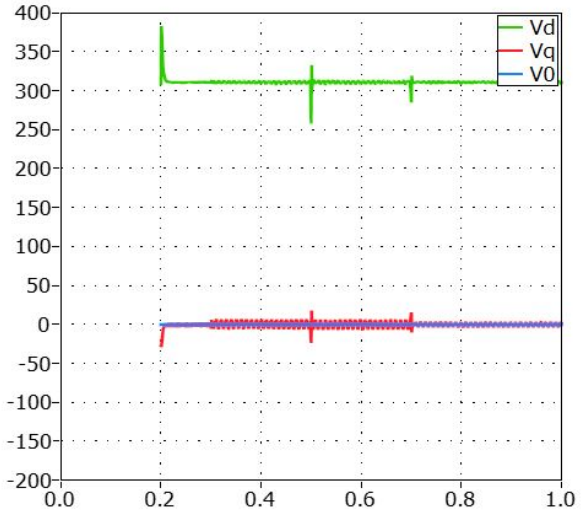

Fig. 8. The following load voltage is compensated on the dq0 coordinate system.

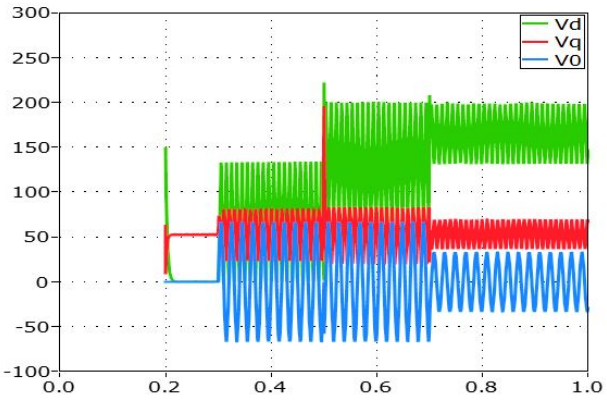

Fig. 9. Signal behind controller.

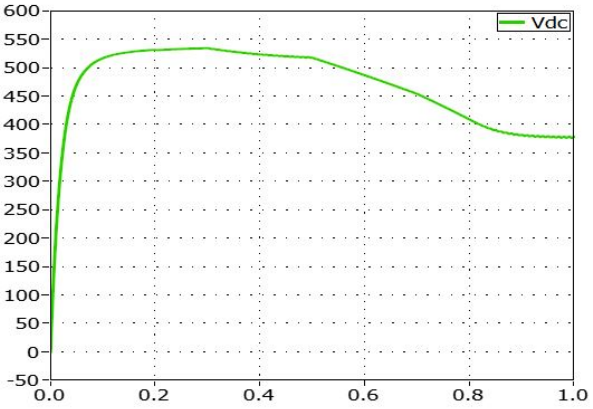

Fig. 10. DC Bus voltage.

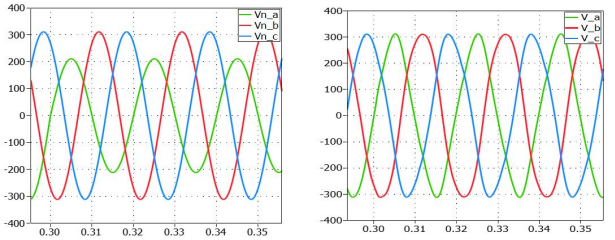

Fig. 11. Mains voltage and voltage after a 1-phase voltage drop compensator.

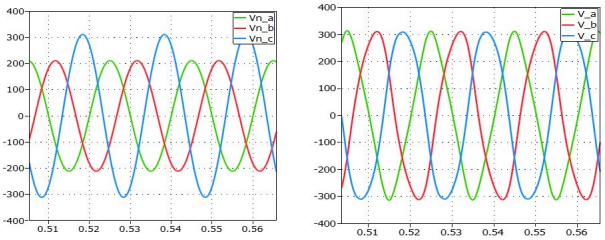

Fig. 12. Mains voltage and voltage after the compensator for a 2-phase voltage drop.

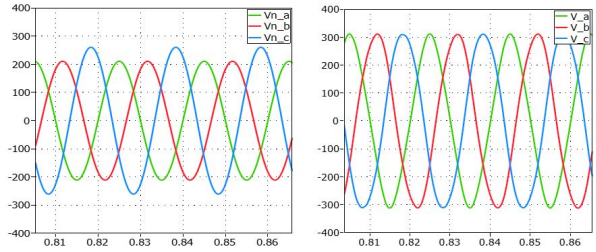

Fig. 13. Mains voltage and voltage after the compensator for a 3-phase voltage drop.

oscillation signal is not stable.

Due to the high-power harmonics present, the voltage compensation of the system is not working well. As a result, voltage peak distortion occurs but still ensures amplitude and frequency for the voltage.

4.2. Case of voltage swell

4.2.1. In case of resistive load R = 100R balanced

In case of sudden 1-phase overvoltage, the system still ensures the output voltage balance reaches the desired value.

4.2.2. In case of nonlinear load (diode bridge)

5. Conclusions

The paper is designed successfully for voltage compensators using a 3-phase 4-branch inverted structure, used in electrical systems or experiencing voltage instability prob-

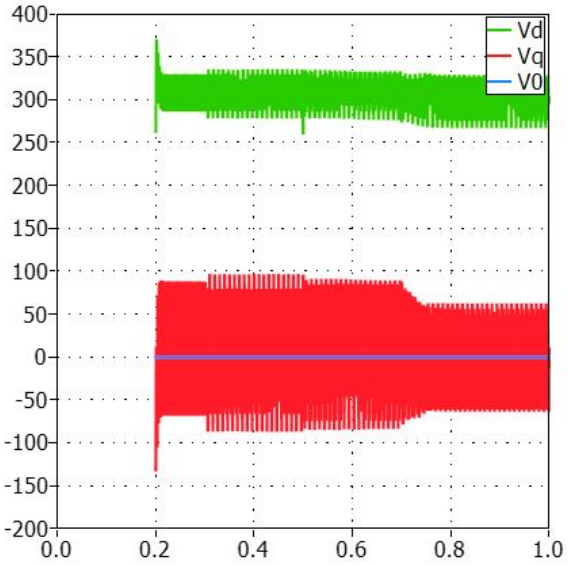

Fig. 14. Drop The following load voltage is compensated on the dq0 coordinate system.

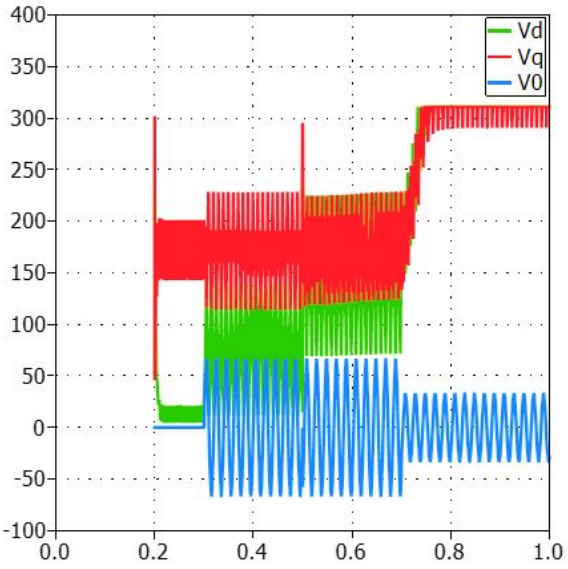

Fig. 15. Signal behind controller.

lems. In this AVC design, the system meets failure detection speed and troubleshooting time requirements on the system's transmission lines. This system reduces short-term voltage fluctuations often appear on the grid during the operation of power plants. The results of this theoretical study are proven by MATLAB simulation. The experiment results will be done in the future to complete the research.

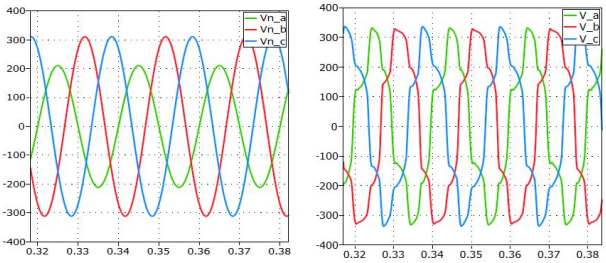

Fig. 16. The mains voltage and the voltage after the compensator in the case of a 1-phase drop.

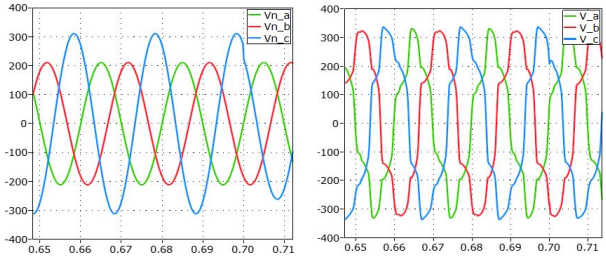

Fig. 17. The mains voltage and the voltage behind the compensator in the case of a 2-phase voltage drop.

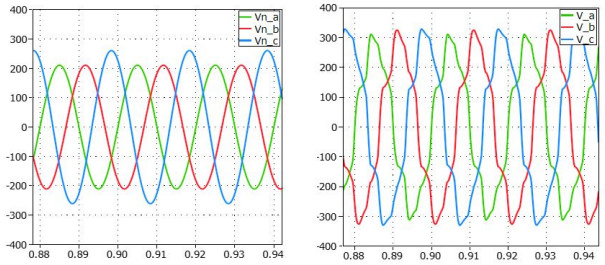

Fig. 18. The mains voltage and the voltage behind the compensator in the case of a 3-phase voltage drop.

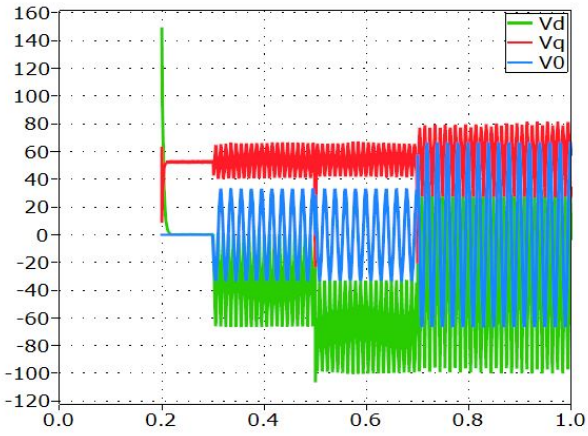

Fig. 19. Signal behind controller.

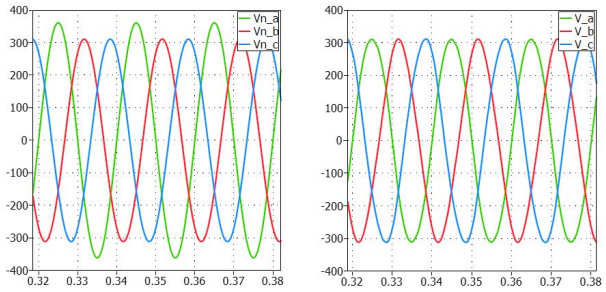

Fig. 20. Mains voltage and voltage after the 1-phase overvoltage compensator.

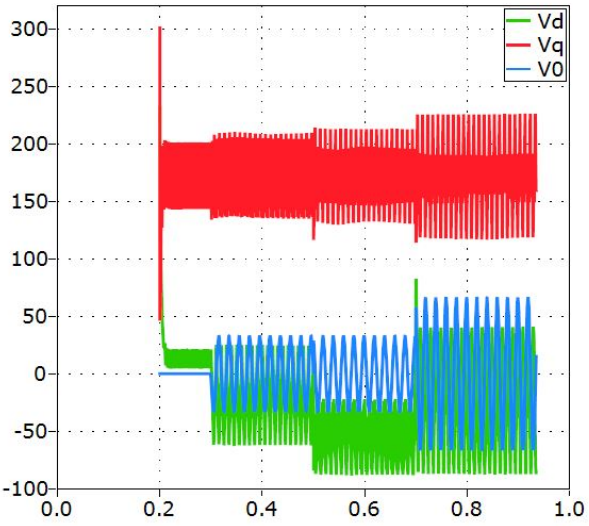

Fig. 21. Signal behind controller.

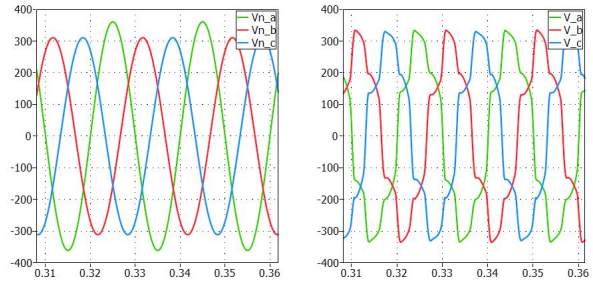

Fig. 22. The mains voltage and the voltage behind the compensator in the case of a 1-phase overvoltage.

Acknowledgments

This research is sponsored by the project at the Hanoi University of Science and Technology.

References

[1] P. Kundur, J. Paserba, V. Ajjarapu, G. Andersson, A. Bose, C. Canizares, N. Hatziargyriou, D. Hill, A. Stankovic, C. Taylor, et al., (2004) *"Definition and classification of power system stability IEEE/CIGRE joint task force on stability terms and definitions"* **IEEE transactions on Power Systems *19***(3): 1387–1401. DOI: 10.1109/TPWRS.2004.825981.

[2] Q. Xu, D. He, N. Zhang, C. Kang, Q. Xia, J. Bai, and J. Huang, (2015) *"A short-term wind power forecasting approach with adjustment of numerical weather prediction input by data mining"* **IEEE Transactions on sustainable energy *6***(4): 1283–1291. DOI: 10.1109/TSTE.2015.2429586.

[3] E. G. Potamianakis and C. D. Vournas, (2006) *"Short-term voltage instability: effects on synchronous and induction machines"* **IEEE Transactions on power systems *21***(2): 791–798. DOI: 10.1109/TPWRS.2006.873022.

[4] A. Fouad and V. Vittal, (1983) *"Power system response to a large disturbance: energy associated with system separation"* **IEEE transactions on power apparatus and systems** (11): 3534–3540. DOI: 10.1109/TPAS.1983.317698.

[5] A. Llamas, J. D. L. R. Lopez, L. Mili, A. Phadke, and J. Thorp, (1995) *"Clarifications of the BCU method for transient stability analysis"* **IEEE Transactions on Power Systems *10***(1): 210–219. DOI: 10.1109/59.373944.

[6] Y. Yu and F. Feng, (1991) *"A study on dynamic security regions of power systems"* **Proceedings of the EPSA 2**(1): 11–21.

[7] A. Priyadi, N. Yorino, M. Tanaka, T. Fujiwara, Y. Zoka, H. Kakui, and M. Takeshita, (2012) *"A direct method for obtaining critical clearing time for transient stability using critical generator conditions"* **European Transactions on Electrical Power 22**(5): 674–687. DOI: 10.1002/etep.597.

[8] T. 2. T. S. P. Criteria. *Technique specification of power system security and stability calculation*. 2013.

[9] S. Q. /. G. 404-2010. *Security and stability of the national grid computing specification*. 2010.

[10] C. Picardi, D. Sgrò, and G. Gioffré. "A new active filtering technique for grid-connected inverters". In: *International Symposium on Power Electronics Power Electronics, Electrical Drives, Automation and Motion*. IEEE. 2012, 900–905.

[11] I. E. Commission et al. *Uninterruptible Power Systems (UPS)-Part 3: Method of Specifying the Performance and Test Requirements*. 2011.

[12] I. E. Commission et al. *Specification for uninterruptible power systems (UPS). Performance Requirements and test methods*. 2011.

[13] A. Karpati, G. Zsigmond, M. Vörös, and M. Lendvay. "Uninterruptible Power Supplies (UPS) for data center". In: *2012 IEEE 10th Jubilee International symposium on intelligent systems and informatics*. IEEE. 2012, 351–355.

[14] H. Yujun and M. Petit. "Active voltage control using distributed generation on distribution networks". In: *2013 IEEE Grenoble Conference*. IEEE. 2013, 1–6.

[15] X. Yang, Y. Yuan, X. Zhang, and P. R. Palmer, (2014) *"Shaping high-power IGBT switching transitions by active voltage control for reduced EMI generation"* **IEEE Transactions on Industry Applications** ***51***(2): 1669–1677. DOI: 10.1109/TIA.2014.2347578.

[16] Y. Wang, P. R. Palmer, A. T. Bryant, S. J. Finney, M. S. Abu-Khaizaran, and G. Li, (2009) *"An analysis of high-power IGBT switching under cascade active voltage control"* **IEEE Transactions on Industry Applications** ***45***(2): 861–870. DOI: 10.1109/TIA.2009.2013595.

[17] Q. Xu, Y. Lin, B. Bao, and M. Chen, (2016) *"Multiple attractors in a non-ideal active voltage-controlled memristor based Chua's circuit"* **Chaos, Solitons & Fractals** ***83***: 186–200. DOI: 10.1016/j.chaos.2015.12.007.

[18] T. C. Lim, B. W. Williams, S. J. Finney, and P. R. Palmer, (2012) *"Series-connected IGBTs using active voltage control technique"* **IEEE Transactions on power Electronics** ***28***(8): 4083–4103. DOI: 10.1109/TPEL.2012.2227812.

[19] X. Yang, Y. Yuan, Z. Long, J. Goncalves, and P. R. Palmer, (2015) *"Robust stability analysis of active voltage control for high-power IGBT switching by Kharitonov's theorem"* **IEEE Transactions on Power Electronics** ***31***(3): 2584–2595. DOI: 10.1109/TPEL.2015.2439712.

[20] X.-y. Chen, X.-j. Lu, and K. Yu. "Studies on the influence of loads on voltage stability in the urban power grid". In: *CICED 2010 Proceedings*. IEEE. 2010, 1–7.